

# Denudation rates of a subequatorial orogenic belt based on estimates of sediment yields: evidence from the Paleozoic Appalachian Basin, USA

Kenneth A. Eriksson and Brian W. Romans

Department of Geosciences, Virginia Tech, Blacksburg, VA, USA

## ABSTRACT

The Upper Mississippian (*ca.* 325 Ma) Pride Shale and Glady Fork Member in the Central Appalachian Basin comprise an upward-coarsening, *ca.* 60-m-thick succession of prodeltaic-delta front, interlaminated fine-grained sandstones and mudstones gradational upwards into mouth-bar and distributary-channel sandstones. Analysis of laminae bundling in the Pride Shale reveals a hierarchy of tidal cycles (semi-diurnal, fortnightly neap-spring) and a distinct annual cyclicity resulting from seasonal fluvial discharge. These tidal rhythmites thus represent high-resolution chronometers that can be used in basin analysis. Annual cycles average 10 cm in thickness, thus the bulk of the Pride Shale-Glady Fork Member in any one vertical section is estimated to have accumulated in *ca.* 600 years. Progradational clinofolds are assumed to have had dips of 0.3–3° with a median dip of 1.7°; the latter infilled a NE-SW oriented foreland trough up to 300 km long by 50 km wide in the relatively short time period of 90 kyr. The total volume of sediment in the Pride basin is *ca.* 900 km<sup>3</sup> which, for an average sediment density of 2700 kg m<sup>-3</sup>, equates to a total mass of *ca.* 2.4 × 10<sup>6</sup> Mt. Thus, mass sediment load can be estimated as 27 Mt yr<sup>-1</sup>. For a drainage basin area of 89 000 km<sup>2</sup>, based on the scale of architectural channel elements and cross-set thicknesses in the incised-valley-fill deposits of the underlying Princeton Formation, suspended sediment yields are estimated at *ca.* 310 t km<sup>-2</sup> yr<sup>-1</sup> equating to a mechanical denudation rate of *ca.* 0.116 mm yr<sup>-1</sup>. Calculated sediment yields and inferred denudation rates are comparable to modern rivers such as the Po and Fly and are compatible with a provenance of significant relief and a climate characterized by seasonal, monsoonal discharge. Inferred denudation rates also are consistent with average denudation rates for the Inner Piedmont Terrane of the Appalachians based on flexural modelling. The integration of stratigraphic architectural analysis with a novel chronometric application highlights the utility of sedimentary archives as a record of Earth surface dynamics.

## INTRODUCTION

Characterizing the relationship of drainage basin denudation to sediment delivery and, ultimately, stratigraphic preservation has important implications for understanding linkages and feedbacks between orogenic belts and global climate and biogeochemical cycles (e.g. Molnar & England, 1990; Willenbring & von Blanckenburg, 2010; Romans & Graham, 2013; Larsen *et al.*, 2014). Various techniques have been used to determine denudation rates of modern and ancient orogenic belts including <sup>40</sup>Ar/<sup>39</sup>Ar, K/Ar and Rb/Sr cooling ages (e.g. Jamieson & Beaumont, 1988; Copeland & Harrison, 1990), fission track dating (e.g. Cerveny *et al.*, 1989; Sorkhabi *et al.*, 1996; Resentini & Malusa, 2012), low-temperature thermochronometry via (U-Th)/He dating (e.g. Zeitler *et al.*,

1987; Carrapa, 2010), and cosmogenic radionuclides (e.g. Portenga & Bierman, 2011; Covault *et al.*, 2013; Granger & Schaller, 2014). A less commonly used approach is based on determinations of sediment volumes and estimates of sediment yields (e.g. Braun, 1989; Poag & Sevon, 1989). Sediment yields on the modern Earth are estimated by measuring solid and solute loads in rivers and normalizing for drainage basin area (e.g. Milliman & Farnsworth, 2011). For ancient sedimentary basins, sediment volumes can be estimated with some degree of confidence from stratigraphic mapping (with outcrop and/or subsurface data) but difficulties arise in estimating the amount of time represented by a specific sediment volume and, more problematical, in estimating the size of the catchment from which the sediment was derived.

The Upper Mississippian Pride Shale and Glady Fork Member in the Central Appalachian Basin present a unique opportunity to estimate sediment yields and denudation rates for a late Paleozoic orogenic belt using the sedimentary record because: (1) the Pride Shale

Correspondence: Kenneth A. Eriksson, Department of Geosciences, Virginia Tech, 1405 Perry St., Blacksburg, VA 24061, USA. E-mail: kaeson@vt.edu

consists of shale, siltstone and fine-grained sandstone that can be equated with the suspended load of the river; (2) sedimentation rates can be accurately estimated from the average thickness of annual tidal-climatic cycles and thus the time represented by the Pride Shale and Glady Fork Member can be determined; (3) sediment volumes can be determined with accuracy from stratigraphic relationships and (4) the thickness of architectural channel elements and cross-set thicknesses in incised-valley deposits beneath, and distributary-channel deposits above the Pride Shale can be used to estimate bankfull discharge and associated drainage basin area.

## GEOLOGIC SETTING

The Pride Shale and Glady Fork Member are preserved in a NE-SW oriented foreland trough (300 km long by 50 km wide) that extends from southern West Virginia to northeastern Tennessee (Fig. 1). Sediment was derived from the Alleghanian fold-thrust belt to the southeast and east (Reed *et al.*, 2005a; Park *et al.*, 2010; Buller, 2014). In West Virginia, the Pride Shale and overlying Glady Fork Member, together with the underlying Princeton Formation comprise an unconformity-bounded, 4th-order depositional sequence of *ca.* 400 kyr duration (Fig. 2; Miller & Eriksson, 2000). The Princeton Formation occupies an incised valley with dimensions of *ca.* 35 km wide by 40 m deep (Fig. 3) and records an upward transition from braided-alluvial to tidal estuarine sedimentation (Miller & Eriksson, 2000). This formation represents the lowstand and transgressive systems tracts of the 4th-order sequence (Fig. 2). Locally, a transgressive ravinement lag deposit separates the Princeton Formation from a black, fossiliferous mudstone at the base of the Pride Shale that is interpreted as the condensed section of the sequence (Miller & Eriksson, 2000). The upward-coarsening Pride Shale and Glady Fork Member average 60 m thick throughout the basin (Fig. 3) and

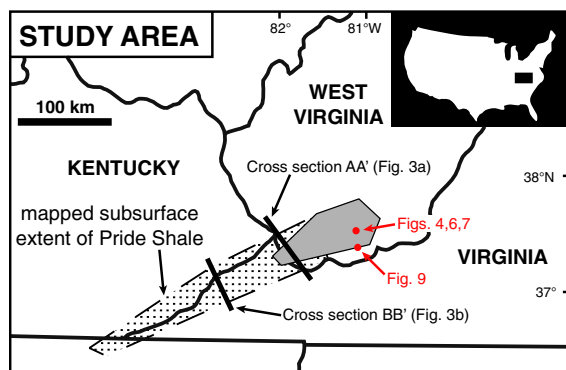


Fig. 1. Map showing distribution of Pride Shale and Glady Fork Member in outcrop in the study area and in the subsurface to the southwest. Note location of cross-sections shown in Fig. 3.

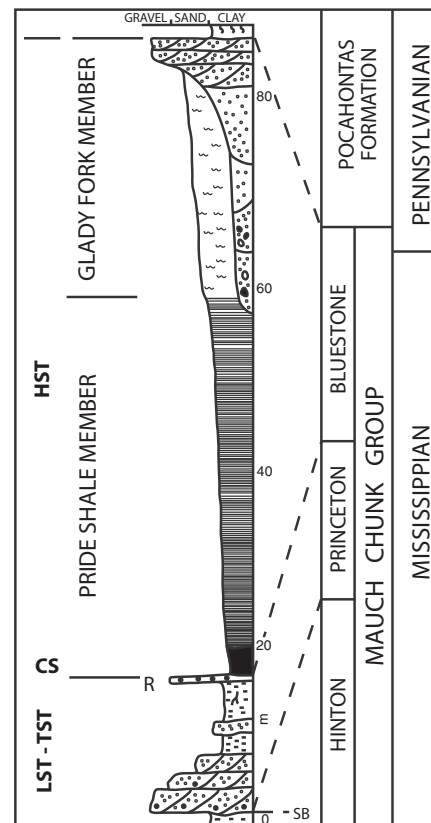


Fig. 2. Stratigraphy of the Princeton-Pride-Glady Fork fourth-order sequence based on expression in outcrop belt of southern West Virginia. SB: sequence boundary; LST: lowstand systems tract; TST: transgressive systems tract; R: transgressive ravinement lag; CS: condensed section; HST: highstand systems tract.

consist of prodeltaic, thinly interlaminated mudstone and fine-grained sandstone overlain by delta front/distributary mouth-bar-channel sandstone and subordinate mudstone (Miller & Eriksson, 1997). Bedding in the Pride Shale is inclined steeper than regional dip, which, together with grain-size trends, are suggestive of southwestward progradation. The Pride Shale and overlying Glady Fork Member represent highstand systems tract deposits (Fig. 2) that accumulated within a maximum duration of 400 kyr (Miller & Eriksson, 2000). Subsurface mapping confirms that the Pride Shale thins to the northwest or is truncated to the northwest beneath the Mississippian-Pennsylvanian unconformity, and is progradational to the southwest as evidenced by an upward-coarsening motif in southern West Virginia and into southwestern Virginia (Fig. 3). The exact nature of the distal equivalents of the Pride Shale, further to the southwest and out of the study area, are unknown; however, the lack of erosional unconformities that could be interpreted as sequence boundaries combined with the overall highstand depositional regime suggests significant basinward bypass was minimal.

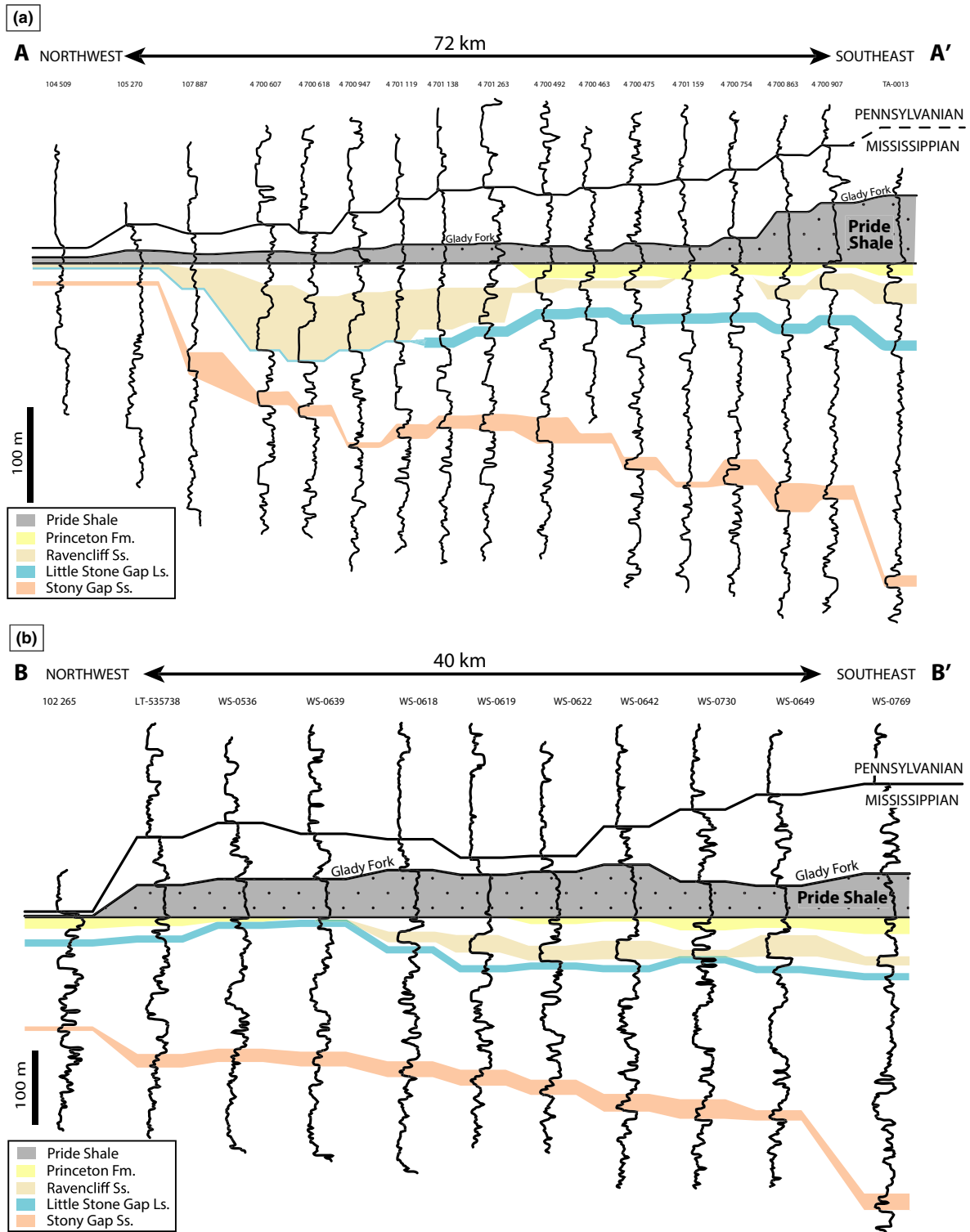


Fig. 3. Well log cross-sections A–A' and B–B' from McDowell and Mingo Counties, southern West Virginia and Wise County, southwest Virginia (refer to Fig. 1 for locations of cross-sections).

Paleogeographic reconstructions (Blakey, 2013) indicate a low paleolatitude (5–10° south of equator). Ubiquitous vertisols and less abundant calcic paleosols within red mudstones of the underlying Hinton Formation and

overlying nonmarine strata of the Bluestone Formation are suggestive of a monsoonal, semi-arid climate at the time of deposition of the Pride Shale (Cecil, 1990; Miller & Eriksson, 1997, 1999).

## TIDAL CYCLICITY AND SEDIMENTATION RATES

The Pride Shale is fully exposed in road cuts along Interstate I-77 in southern West Virginia and displays a distinctive corrugated weathering pattern in outcrop (Fig. 4). Bioturbation is noticeably absent in the Pride Shale and is attributed to rapid rates of sedimentation coupled with anoxic bottom waters (Miller & Eriksson, 1997).

The Pride Shale preserves a hierarchy of submillimeter- to decimetre- to meter-scale cycles (Fig. 5; Miller & Eriksson, 1997). The lowest level of the hierarchy consists



Fig. 4. Characteristic corrugated outcrop pattern of the Pride Shale at Camp Creek roadcut along I-77, southern West Virginia.

of submillimeter-thick, normally graded, fine-grained sandstone-black mudstone or siltstone-black mudstone couplets; thick-thin pairs of laminae rarely are preserved (Fig. 6a). Up to 17 couplets are stacked into systematically upward-thickening and thinning millimetre- to centimetre-scale cycles (Fig. 6b). Up to 18 of these cycles are arranged in upward-thickening and thinning decimetre-scale cycles (Fig. 6b) that are manifested as the corrugations in outcrop (Figs 4, 6c). These cycles consist of interbedded, positive-weathering, more arenaceous facies and negative-weathering, more argillaceous facies. Meter-scale, multiyear cycles consist of 17–22 annual beds that display a crude upward thickening and thinning (Miller & Eriksson, 1997). The proportion of sandstone to mudstone systematically increases upward with an average sandstone/mudstone ratio of approximately 50% for the overall succession (refer to Figs 4 and 6).

The hierarchy of cycles preserved in the Pride Shale is interpreted to record a spectrum of tidal and climatic periodicities that can be used as high-resolution chronometers from which sedimentation rates can be estimated (Fig. 5; Miller & Eriksson, 1997). Individual graded sandstone-siltstone laminae are interpreted as suspension fall-out deposits from river plumes generated by the dominant (semi-diurnal) ebb tide. The rarely preserved pairs of laminae are considered to represent the deposits of both the dominant and subordinate diurnal ebb tides. Shale partings separating graded laminae (Fig. 6a) are interpreted as slack-water suspension deposits. Such systematic alternation of relatively thick and thin laminae is observed in modern tidal deposits and uniquely records the diurnal inequality of the tides through its influence on the strength of successive semi-diurnal tidal currents (e.g. de Boer *et al.*, 1989; Dalrymple *et al.*, 1991; Kvale & Archer, 1991). Similar rhythmic sand-mud

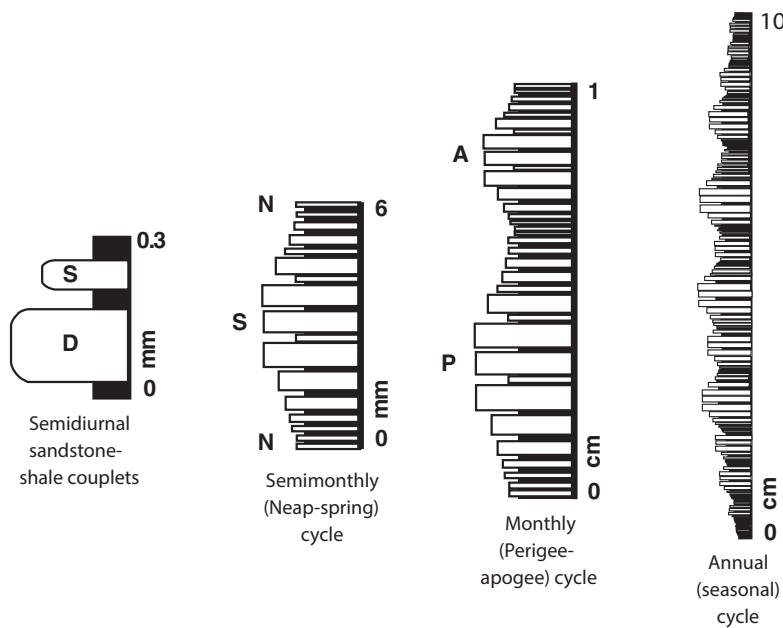
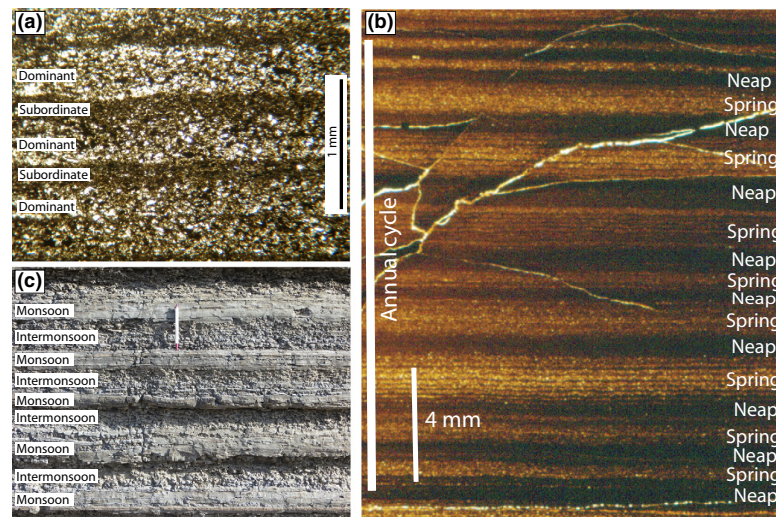


Fig. 5. Idealized representation of hierarchical bundling patterns of laminae in the Pride Shale (modified from Miller & Eriksson, 1997)



**Fig. 6.** (a) Photomicrograph of dominant semi-diurnal sandstone-siltstone/shale couplets with one example of a thick–thin diurnal pair representing the dominant and subordinate ebb tides of the day; (b) Photomicrograph of microlaminated, neap–spring–neap cycles from Spanishburg outcrop, southern West Virginia. Cycles typically consist of 15 or fewer distinct sandstone-siltstone/shale couplets. Each sandstone-siltstone lamination represents a semidiurnal deposit of the dominant ebb tide of each day. Rarely preserved are the deposits of the subordinate tide of the day. Annual cycles consist of systematic thickening and thinning of between 11 and 18 neap–spring–neap cycles; (c) Decimetre-scale annual cycles at roadcut along I-77, southern West Virginia. Each furrow-rib-furrow contains up to 18 neap–spring–neap cycles. Annual cycles reflect climatic changes in which thicker, coarser laminae record seasonal monsoonal conditions when fluvial input was enhanced because of increase terrestrial runoff and thinner, finer-grained laminae record intermonsoonal conditions when sediment flux was less (pen for scale is 15 cm long).

alternations are present in the delta front/prodelta settings of the Fly River, Yangtze, and Amazon deltas on millimetre to centimetre scales (Jaeger & Nittrouer, 1995; Hori *et al.*, 2002; Dalrymple *et al.*, 2003; Harris *et al.*, 2004). In addition, rhythmites of the Neoproterozoic Reynella Siltstone and parts of the Elatina Formation in South Australia similarly display laminae that are arranged in thick–thin pairs (Williams, 1989, 1991). Thickening and thinning, millimetre- to centimetre-scale cycles in the Pride Shale are considered to represent fortnightly, neap–spring tidal deposits. These cycles are comparable to neap–spring cycles that occur in modern tidal deposits (e.g. Dalrymple *et al.*, 1991; Tessier, 1993; Greb *et al.*, 2011). A comparable neap–spring signal is discernable in the tidal laminites of the Amazon delta (Jaeger & Nittrouer, 1995). Similar thickening and thinning cycles in the Neoproterozoic Elatina Formation are up to 2 cm thick and contain 8–16 laminae. The abbreviated character of the neap–spring cycles in the Pride Shale is inferred to be a reflection of the relatively distal, prodeltaic setting in which deposition took place and into which not only the subordinate daily flows but also the weakest neap ebb flows were of insufficient strength to transport sand. Decimetre-scale cycles in the Pride Shale are interpreted to record an annual climatic (monsoonal) signal in which thicker neap–spring cycles record the monsoon when voluminous sediment was supplied to the river mouth and the thinner cycles record the inter-monsoon when less sediment was supplied to the delta (Miller & Eriksson, 1997). Maximum entropy spectral analysis on the

decimetre-scale cycles reveals a strong peak at 16.7 neap–spring cycles (Miller & Eriksson, 1997). Annual cycles in the Pride Shale range in thickness from <3 cm at the base to as much as 50 cm at the top and correspond with the upward increase in sandstone/mudstone ratio. The average thickness of annual cycles is estimated as *ca.* 10 cm (Figs 4, 6c). Meter-scale cycles are interpreted by Miller & Eriksson (1997) to represent 18.6 year nodal cycles in which thicker annual beds developed during times when the inclination of the lunar orbital plane favoured an increase in tidal amplitudes. The overlying Gladly Fork Member also displays evidence of sedimentation under the influence of tides in the form of wavy and flaser bedding (Miller & Eriksson, 2000).

## COMPLETENESS OF THE STRATIGRAPHIC RECORD

The literature is replete with arguments that the stratigraphic record is more incomplete than complete and represents merely a set of ‘frozen accidents’ (e.g. Baily & Smith, 2010). Stratigraphic incompleteness is evident at all timescales, but becomes especially important at longer durations ( $\geq 10^6$  yr) as hiatuses that span multiple timescales accumulate in the record (Plotnick, 1986; Miall, 2015). Thus, an assessment of the continuity of the stratigraphic succession used in this study is warranted. Photo-mosaic mapping of road-cut exposures of the prodeltaic Pride Shale in southern West Virginia reveals no signifi-

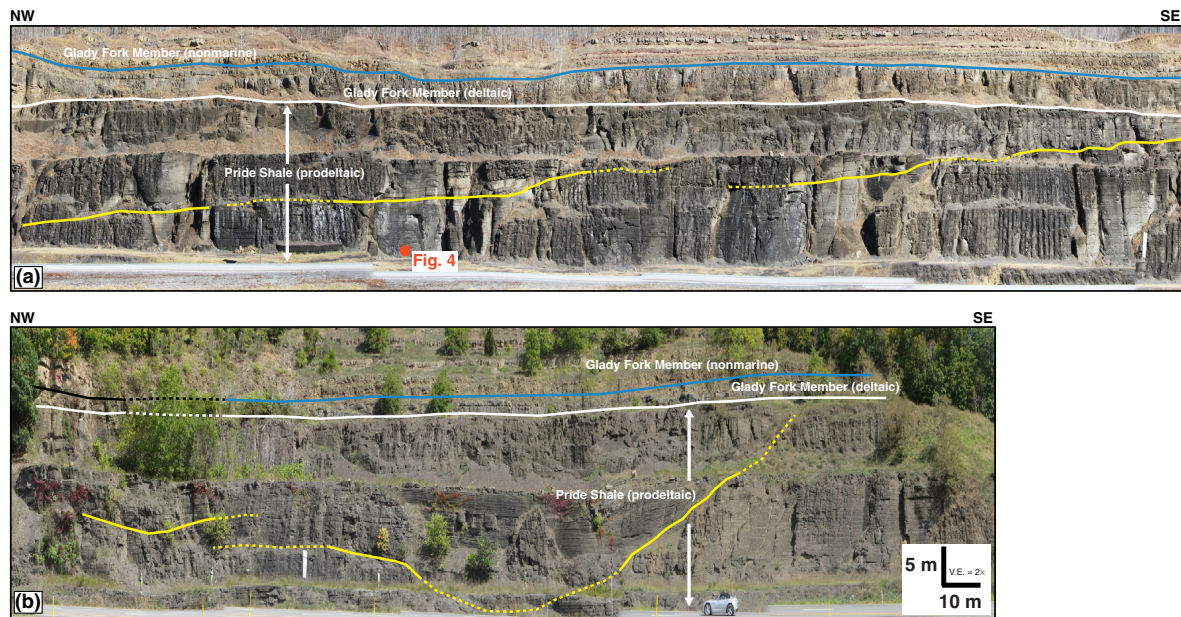


Fig. 7. Photomosaics of Bluestone Formation outcrops northwest of Camp Creek exit off Interstate-77 in southern West Virginia (lat: 37.502055; long: -81.109160). Mosaic A shows a part of southeastern road cut and Mosaic B shows the northwestern road cut. Scale is the same for both panels. Yellow lines within Pride Shale Member denote discontinuities that are interpreted as slump-scar surfaces. Approximate location of Fig. 4 is highlighted.

cant hiatuses in sedimentation (Fig. 7). The surfaces of discontinuity that traverse parts of the outcrop (Fig. 7) are interpreted as slump scars related to rapid sedimentation and over-steepening of deltaic clinoforms rather than products of erosion (Miller & Eriksson, 1997). The Pride Shale at this outcrop is interpreted to record effectively continuous sedimentation but at different rates over different time scales based on the recognition of tidal hierarchies discussed above. At the shortest or diurnal time scale preserved in the Pride Shale, inferred dominant, ebb-tide sand-silt micro-laminae record the most rapid diurnal rates of sedimentation, whereas the deposits of the majority of subordinate ebb tides as well as the flood-tides are preserved in mudstone drapes that record slower rates of sedimentation (Figs 5, 6a, b). Within neap-spring cycles, as noted above, the spring-tide record is well preserved but the neap-tide records are incomplete and likely are preserved in mudstone-dominated intervals that record slow, suspension sedimentation (Figs 5, 6b). Annual cycles similarly preserve a record of variable sedimentation rates in which monsoonal facies are preserved in the form of stacked neap-spring cycles that record the most rapid rates of sedimentation during the year. In contrast, intermonsoonal facies are dominated by mudstone intervals that reflect six or more fortnights of slow, suspension sedimentation (Figs 5, 6b). Decadal cycles in the Pride Shale also preserve a record of variable sedimentation rates with up to half of the nodal record preserved in mudstone intervals. Notwithstanding the evidence for variable rates of sedimentation, the Pride Shale preserves an uninterrupted record from which average annual sedi-

mentation rates can be extracted over decadal timescales. Cyclicity is not apparent in the flaser- and wavy-bedded, mouth-bar facies of the overlying Glady Fork Member but evidence for major hiatuses also is lacking in this facies.

The issue of whether this expression of remarkably continuous sedimentation at the outcrop is representative of the Pride Shale over the entire depocentre introduces uncertainty into the methods of this study. The generally consistent gamma-ray log expression of the Pride Shale in the subsurface (Fig. 3) suggests that the style of deposition is similar over much of the depocentre. However, to address the potential for hiatuses beyond what can be characterized in outcrop, a maximum total duration of 400 kyr is used as a conservative limit in the calculations of sediment yield and denudation. An additional consequence of the time-varying completeness of the stratigraphic record is that it can result in misleading extrapolation of process rates across timescales (Sadler, 1981; Sadler & Jerolmack, 2015). This issue is addressed below within the context of the specific methods used to estimate sediment yields and denudation rates.

## ESTIMATING SEDIMENT YIELDS AND DENUDATION FROM ACCUMULATION RATES

The total duration of deposition is required to calculate sediment load and yield and was determined by combining the tidal-rhythmite-constrained linear sedimentation rate ( $10 \text{ cm yr}^{-1}$ ) with deltaic clinoform geometry. The

overall coarsening-upward pattern of the Pride Shale is consistent across the 15 000-km<sup>2</sup> depocentre and interpreted to record basinward (southwestward) progradation of the Pride-Glady Fork delta system (Fig. 3). The lack of coarse-grained (i.e. medium-grained sand and coarser) deposits within the Pride Shale indicates that coarse-grained material was trapped on the topset, whereas mud to fine-grained sand was delivered to the clinoform foreset throughout basin filling. Additionally, the lack of erosional unconformities within the Pride Shale indicates that bypass of sediment to distal reaches was negligible. In this depositional model, the duration of basin filling is, in part, a function of the clinoform dip. Establishing a range of plausible clinoform dips and, thus, a range of total duration of sediment accumulation in the depocentre, captures some of the inherent uncertainty with determining time in ancient sedimentary systems.

The gently inclined bedding surfaces in the Pride Shale are interpreted as clinoforms but it is impossible to measure explicitly the foreset slopes due to lack of km-scale dip-parallel outcrops. However, ancient and modern analogues provide a plausible range of foreset slopes. The prodelta region of the Holocene Huanghe (Yellow River) delta is similar to the Pride delta system in terms of clinothem thickness and dominant grain size on the foreset (Liu *et al.*, 2004). The foreset slopes on the Huanghe are generally very low (<0.1°; Liu *et al.*, 2004), but locally are up to 0.4° (Prior *et al.*, 1986). The presence of well-exposed stratal discontinuities interpreted as slump scars (Fig. 7) (Miller & Eriksson, 1997) suggest that Pride delta slopes were likely >0.1°. Prior *et al.* (1986) documented gullied depressions and associated mass-transport deposits on the Huanghe prodelta at slopes of 0.3–0.4°. A minimum clinoform angle is therefore set at 0.3°. Compilations of clinoform slopes from outcropping and subsurface examples of large-scale (100–1000's of meters of relief) shelf-slope systems indicate a range of 2–5° (e.g. Hubbard *et al.*, 2010); however, delta-scale clinoforms with 10s of meters of relief typically have average slopes <3° (Olariu *et al.*, 2010). A morphometric analysis of 20 modern delta-scale subaqueous clinoforms by Patruno *et al.* (2015) subdivides systems into 'mud-prone' and 'sand-prone', with muddy systems having low average foreset gradients (<0.8°) and sandy systems with average slopes >0.4° and including some slopes much steeper (up to 6°). However, it is difficult to compare the Pride system, which is *ca.* 50% fine-grained sandstone and *ca.* 50% mudstone overall, to the qualitative mud-prone vs. sand-prone classification of Patruno *et al.* (2015). A maximum foreset angle for the mixed mud-sand Pride system is therefore set to 3° in order to conservatively capture the range of plausible scenarios. On the sediment load and yield plots (Fig. 8), the median clinoform dip (1.7°) case is shown by the symbol with the computed minima and maxima represented by *y*-axis error bars.

Based on a sedimentation rate of 10 cm yr<sup>-1</sup>, any 60-m-thick section of Pride Shale and Glady Fork Member represents *ca.* 600 years. With a median clinoform dip of

1.7°, deltaic progradation would have infilled the 300-km-long basin in *ca.* 90 kyr, well within the inferred 400 kyr duration of the 4th-order Princeton-Pride-Glady Fork sequence (Miller & Eriksson, 2000). For the purposes of this discussion, the cross-sectional area of the Pride-Glady Fork basin is modelled with a height of 60 m, corresponding with the thickness of the Pride Shale and Glady Fork Member, and a base of 50 km, corresponding with the width of the basin. For a 300-km-long basin, the volume of sediment is estimated as *ca.* 900 km<sup>3</sup>. Using an average sediment density of 2700 kg m<sup>-3</sup>, the total sediment mass is *ca.* 2.4 × 10<sup>6</sup> Mt. Based on the median time represented by the Pride Shale and Glady Fork Member, sediment load is, therefore, estimated as 27 Mt per year (Fig. 8a).

There is the potential for uncertainty related to using sediment accumulation rates derived from one timescale as representative of another timescale (Sadler, 1981; Miall, 2015). In this case, the tidal-rhythmite-constrained rates (sub-annual to decadal) are extrapolated to centennial (10<sup>2</sup> yr) timescales, and then inferred to be maintained at 10<sup>4</sup>–10<sup>5</sup> yr timescales (i.e. the time to prograde and fill the depocentre). However, in order to address the possibility of 'more gap than record' in this analysis, the maximum inferred duration of 400 kyr, which is up to 25 times longer than estimated durations, is incorporated into the calculations (Fig. 8). Also worth noting is a recent global compilation and analysis by Sadler & Jerolmack (2015) that emphasized the importance of mapping sediment volumes (as opposed to just thickness) and using rates derived from stratigraphic successions down-system from the fluvial transfer zone, both of which are done in this study. Sadler & Jerolmack (2015) concluded that upland denudation rates determined from sediment yields show little or no dependence of rate on time interval with such an approach. Another uncertainty worthy of consideration is to what extent lateral avulsion of delta lobes via autogenic dynamics (e.g. Hoyal & Sheets, 2009) has on the estimation of total duration of the depocentre. In this case, the relatively narrow (*ca.* 50 km) foreland trough precluded significant lateral switching that might have generated adjacent stratigraphic packages of wholly different ages. Longshore drift of sediment also could have an influence on estimates of total duration of the depocentre. Evidence in the rock record for longshore drift, such as beach deposits, is lacking. Furthermore, longshore drift is not considered to have been a significant factor because of the rapid progradation of the delta. The large range of plausible durations used here is considered to capture any potential variability driven by longshore drift or autogenic processes such as delta switching.

Sediment yields for modern rivers are normalized for drainage basin area to permit comparison of rivers but estimating the size of ancient (unpreserved) drainage basins is difficult. One approach is to use the scale of architectural fluvial elements in the underlying Princeton Formation and the overlying Glady Fork Member as a proxy for drainage basin area using the empirical relation-

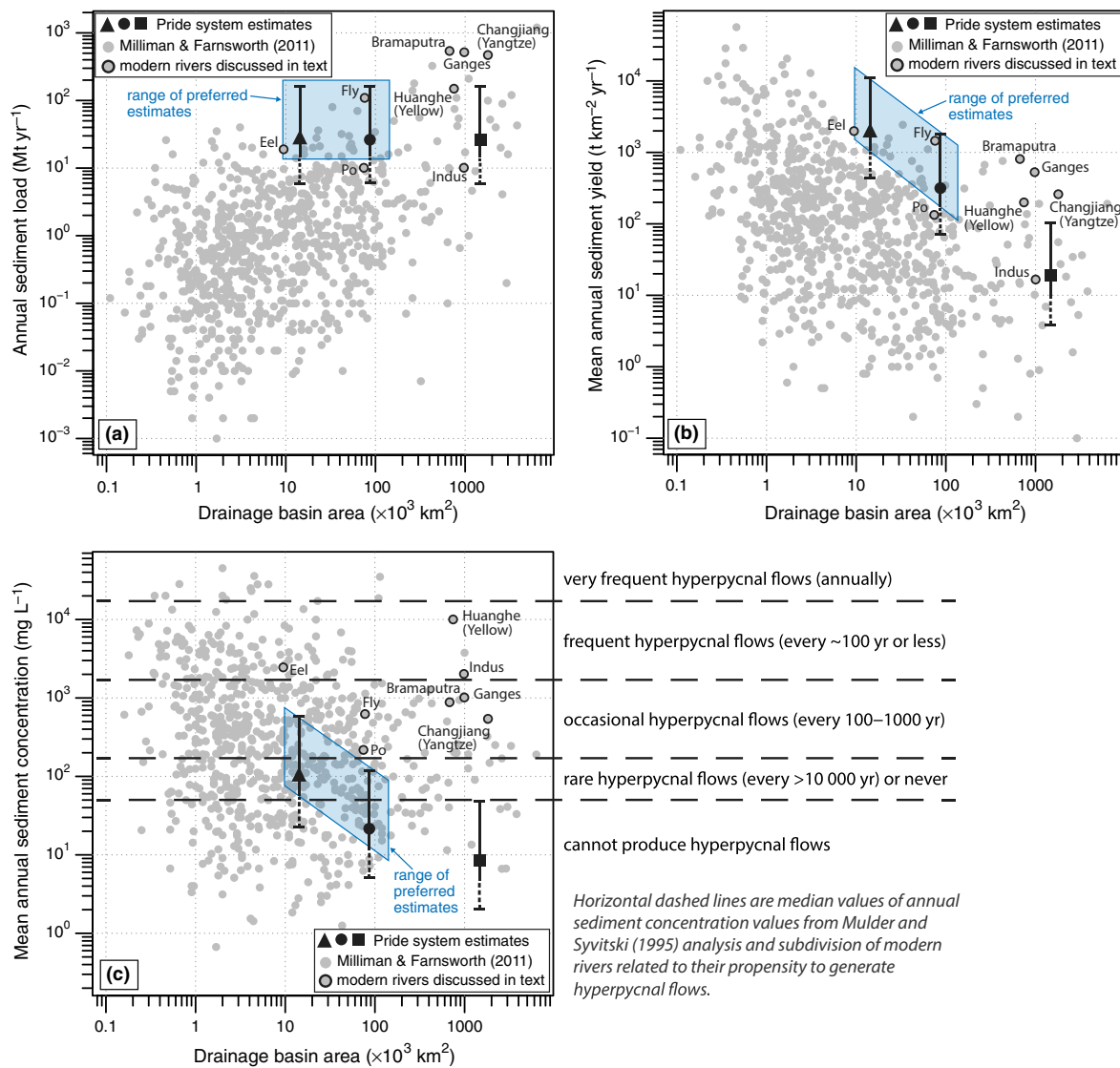


Fig. 8. Estimates of Pride river system in terms of: (a) annual sediment load; (b) mean annual sediment yield; and (c) mean annual suspended sediment concentration in comparison to global database of modern rivers from Milliman & Farnsworth (2011). Part C compares results to the hyperpycnal-flow frequency subdivision of Mulder & Syvitski (1995). Error bars in the y-axis direction represent a range of durations for filling the depocentre; solid line and maxima represent estimated durations, whereas dashed line extending downward to the minima represents the maximum duration of the Pride Shale (400 kyr). The range in the x-direction represent a range of catchment area estimates. The regions of favoured estimates are shown by the blue polygons. See text for further explanation of range of uncertainties and for discussion of modern rivers shown.

ship used by Davidson & North (2009),  $d = aDA^b$ , where ( $d$ ) is bankfull depth or discharge, ( $DA$ ) is drainage basin area, and coefficient ( $a$ ) and exponent ( $b$ ) are region-specific variables dependent on climate, location and lithology, and that represent a 'regional hydraulic geometry curve' obtained from modern catchment surveys. The Princeton and Gladly Fork fluvial facies consist of stacked, erosively based channel elements (Fig. 9) that range in thickness from 0.25 to 3.60 m (Table 1; Table S1). Paola & Bergman (1991) proposed that the average ratio of preserved element thickness to mean bankfull depth is roughly 0.67 (average of range of 0.55–0.78). Using this method, the maximum bankfull depth for the Princeton river system

is, thus, computed to be 5.4 m (Table 2). An alternative approach to calculating bankfull depths is based on the relationship between dune height and mean set thickness of medium-scale cross-strata in fluvial sandstones and the known relationship between dune height and water depth (Bridge & Tye, 2000). Mean cross-set thicknesses in fluvial, coarse-grained sandstones of the Princeton Formation are 35 cm (Table 1; Table S1). Using the empirical equations of Bridge & Tye (2000) and references therein, dune height is estimated as 1.1 m and bankfull depth as 6.1 m. These independent estimates of bankfull depth are sufficiently similar that, for purposes of this study, an average depth of 5.8 m for the Princeton river system is



Fig. 9. Stacked, erosively based, fluvial channel elements in the Princeton Formation at the Athens exit of Interstate-77 in southern West Virginia (lat: 37.424322; long: -81.066375). Dashed lines denote element boundaries. Person for scale in foreground is 1.9 m.

Table 1. Fluvial channel element and cross-set thickness data summary

	Minimum	Median	Mean	Maximum	Standard deviation
Princeton $F_m$ incised-valley-fill channel element thickness ( $n = 31$ )	0.25	1.80	1.83	3.60	0.81
Glady Fork $F_m$ deltaic distributary-channel element thickness ( $n = 7$ )	1.52	2.79	2.40	3.05	0.60
Princeton $F_m$ cross-set thickness ( $n = 35$ )	0.20	0.30	0.35	0.80	0.14

used (Table 2). Because of the close agreement (12% difference) between the two calculation methods, an estimate of bankfull depth of 4.6 m for the Glady Fork river system is based only on thicknesses of channel elements (Table 2).

A regional hydraulic curve that ideally matches conditions in the Late Mississippian Central Appalachian Basin is not available. However, an example from the Western Cordillera of the US Pacific Northwest coast (Castro & Jackson, 2001) compares favourably (scenario 'B' in Table 2). The climate for this regional curve is characterized by a combination of dry summer continental climates, with seasonal precipitation, and humid continental climates with no dry season. Based on this curve, the estimated maximum drainage basin area for the Princeton Formation incised-valley deposits equates to *ca.* 87 000 km<sup>2</sup> (Table 2). However, in order to capture a plausible range of paleoclimatic conditions, two additional regional curves are used, which result in drainage basin area estimates as low as *ca.* 14 000 km<sup>2</sup> and as high as *ca.* 1 500 000 km<sup>2</sup> (Table 2). The estimates of drainage basin areas based on the Glady Fork architectural elements (Table 2) are considered to be minima as the exposed channel deposits likely represent deltaic distributary channels and not the trunk river system (see Blum *et al.*, 2013; Holbrook & Wanas, 2014).

Assuming a drainage basin area of *ca.* 87 000 km<sup>2</sup> and the median clinoform dip, the suspended sediment yield of the Pride delta system can be estimated at *ca.* 310 t km<sup>-2</sup> yr<sup>-1</sup> (Table 3; Fig. 8b). Sediment yields can be converted to a volume equivalent by dividing the mass of the material by the average density of bedrock (2700 kg m<sup>-3</sup>). The calculated volume of sediment carried by the river can be equated with the change in form of the ground surface. Assuming little to no sediment

accumulation in areas outside of the mapped area, the volume change is equivalent to a mean rate of ground surface lowering (denudation). The estimated sediment yields for the likely Pride Shale drainage basin scenario results in denudation rates of 0.06–0.66 mm yr<sup>-1</sup> (with a likely value of 0.116 mm yr<sup>-1</sup>) for the orogenic terrane from which the sediment was derived (Table 3). An unknown amount of sediment storage in depositional segments updip of the mapped deltaic accumulation (e.g. in fluvial floodplains) would result in minimum denudation rate estimates. However, the preferred small to moderate drainage basin area scenarios (rationale discussed below), which have minimal to negligible onshore sediment storage over  $\geq 10^4$  yr timescales (Metivier & Gaudemer, 1999; Castelltort & van den Driessche, 2003; Allen, 2008; Romans *et al.*, 2015), means the subaqueous delta depocentre is a faithful recorder of source-to-sink mass transfer.

The analysis of sediment load/yield and paleodrainage basin area also permits investigation of the potential for an ancient river system to generate hyperpycnal flows. A marine hyperpycnal plume occurs when the suspended sediment concentration at the river mouth is sufficiently large to create a flow with a density greater than sea water that, in turn, can generate a turbidity current (Mulder & Syvitski, 1995). Such underflows have the potential to erode the prodeltaic substrate and generate deposits with highly variable spatial distribution (Mulder *et al.*, 2003), which could complicate the ability to use the tidal-rhythmite-dominated stratigraphic volume as a proxy for duration. We calculated the mean annual suspended sediment concentration for the Pride–Glady Fork scenarios (Table 3) and compare them to the hyperpycnal-flow frequency subdivision of modern rivers by Mulder & Syvitski (1995) (Fig. 8c). In general, smaller drainage basins

Table 2. Fluvial architectural element data, modern regional curve explanation and bankfull depth/discharge parameters used, and resultant estimates of drainage basin areas and discharges

Formation/ Member	Max paleo-channel depth*(m)	Paleo-channel depth†(m)	Average paleo-channel depth (m)	Modern regional curve scenario	Modern regional curve location	Climate classification and description‡	Regional curve parameters§			
							Bankfull depth	Discharge	Estimated drainage area (km <sup>2</sup> )	
Princeton	5.4	6.1	5.8	1A	Pacific Maritime Mts of US Pacific Northwest coast (Castro & Jackson, 2001)	Combination of cool Mediterranean (Csb) seasonal climates and Maritime Temperate (Cfb) with no seasonal variation in precipitation	$a = 0.66$ $b = 0.39$	$a = 91.05$ $b = 0.67$	14 284	8918
				1B	Western Cordillera of US Pacific Northwest coast (Castro & Jackson, 2001)	Combination of Dry Summer Continental climates with seasonal precipitation (Dsa, Dsb, Dsc) to Humid Continental with no dry season (Dfb, Dfc)	$a = 0.61$ $b = 0.33$	$a = 17.28$ $b = 0.86$	86 861	41 079
				1C	Western Interior Basin and Range of US Pacific Northwest coast (Castro & Jackson, 2001)	Semi-Arid, Steppe (BSk) climate with seasonal precipitation	$a = 0.79$ $b = 0.24$	$a = 13.05$ $b = 0.77$	1 472 285	107 362
Glady Fork	4.6	–	4.6	2A	Pacific Maritime Mts of US Pacific Northwest coast (Castro & Jackson, 2001)	Combination of cool Mediterranean (Csb) seasonal climates and Maritime Temperate (Cfb) with no seasonal variation in precipitation	$a = 0.66$ $b = 0.39$	$a = 91.05$ $b = 0.67$	7899	5996
				2B	Western Cordillera of US Pacific Northwest coast (Castro & Jackson, 2001)	Combination of Dry Summer Continental climates with seasonal precipitation (Dsa, Dsb, Dsc) to Humid Continental with no dry season (Dfb, Dfc)	$a = 0.61$ $b = 0.33$	$a = 17.28$ $b = 0.86$	43 125	22 496
				2C	Western Interior Basin and Range of US Pacific Northwest coast (Castro & Jackson, 2001)	Semi-Arid, Steppe (BSk) climate with seasonal precipitation	$a = 0.79$ $b = 0.24$	$a = 13.05$ $b = 0.77$	562 157	51 155

\*0.67 correction factor of Paola &amp; Bergman (1991) applied to maximum measured channel element thickness.

†Empirical equations of Bridge &amp; Tye (2000) and Allen (1970) applied to mean cross-bed set thickness.

‡Köppen climate symbols are as follows: Af, Tropical rainforest; Am, Tropical monsoon; Aw, Tropical savannah; BW, Arid Desert; BS, Arid Steppe-subscripts h and k refer to hot and cold respectively; Cs, Temperate dry summer; Cw, Temperate dry winter; Cf, Temperate without dry season-subscripts a, b and c refer to hot summer, warm summer and cold summer respectively; Ds, Cold dry summer; Dw, Cold dry winter; Df, Cold without dry season-subscripts a, b, c and d refer to hot summer, warm summer, cold summer and very cold winter respectively; ET, Polar Tundra; EF, Polar Frost.

§The coefficient (a) and exponent (b) are quoted in the original source and were computed for imperial units of measure; results have been converted to metric units.

**Table 3.** Sediment load, sediment yield, suspended sediment concentration and denudation rate estimates for Pride–Glady Fork river system and several modern rivers from Milliman & Farnsworth (2011) for comparison

River system	Drainage basin area (10 <sup>3</sup> km <sup>2</sup> )	Sediment load (Mt yr <sup>-1</sup> )	Sediment yield (t km <sup>-2</sup> yr <sup>-1</sup> )	Suspended sediment concentration* (mg L <sup>-1</sup> )	Denudation rate† (mm yr <sup>-1</sup> )
Pride–Glady Fork* [drainage basin estimate A]	14	15–155 (27)	1082–10 830 (1910)	55–550 (97)	0.401–4.011 (0.708)
Eel	10	19	2000	2468	1.000
Pride–Glady Fork* [drainage basin estimate B]	87	15–155 (27)	178–1781 (314)	12–119 (21)	0.066–0.660 (0.116)
Po	74	10	135	217	0.068
Fly	76	110	1447	611	0.724
Pride–Glady Fork* [drainage basin estimate C]	1470	15–155 (27)	10–105 (19)	5–46 (8)	0.004–0.039 (0.007)
Brahmaputra	670	540	806	857	0.403
Huanghe (Yellow)	750	150	200	10 000	0.100
Indus	980	10	10	2000	0.005
Ganges	980	520	531	1061	0.266
Changjiang (Yangtze)	1800	470	261	522	0.131

\*Ranges for Pride–Glady Fork river systems based on range of deltaic clinoform dips, which influences duration of basin filling estimates. Value in parentheses corresponds to median clinoform dip scenario of 1.7°. Refer to text for further explanation.

†Bedrock density of 2700 kg m<sup>-3</sup> used for Pride and density of 2000 kg m<sup>-3</sup> used for modern rivers (per Milliman & Farnsworth, 2011) to convert sediment masses to volumes.

are more prone to generate frequent (every  $\leq 100$  yr) hyperpycnal flows. However, our estimates show that even the smallest drainage basin and highest sediment–yield scenario for the Pride–Glady Fork system falls within the ‘occasional’ (every 100–1000 yr) frequency class (Fig. 8c), which supports outcrop observations that the Pride Shale lacks turbidity current deposits.

An analysis of sediment yields in the geologic record requires an assessment of uncertainties in the calculated sediment volumes, corrections for biogenic carbonates and porosity, the assumption that the sediment was supplied to the basin of deposition in a suspended state, and the implications of excluding dissolved loads from the sediment–yield calculations. The estimate of suspended sediment yields, based on preserved sediment volumes of the Pride Shale and Glady Fork Member, are likely to be a minimum because the package is interpreted to be truncated by the Mississippian–Pennsylvanian unconformity to the west (Englund & Thomas, 1990). However, subsurface mapping demonstrates that the Pride Shale and Glady Fork Member thin westwards and that the present western edge of the structural basin approximates the original margin the depocentre (Buller, 2014). No corrections are necessary for biogenic carbonates or porosity. Calcareous fossils are a minor constituent in the Pride Shale and are confined almost entirely to the basal condensed section and fluid inclusion and vitrinite reflectance data from overlying Early Pennsylvanian strata (Reed *et al.*, 2005b) imply that Pride Shale was buried to at least 4 km depth such that all porosity was destroyed by compaction. The assumption that sediment was transported as suspended load is supported by the overall fine grain size in the Pride Shale and conclusions of Miller &

Eriksson (1997) that all sediment was deposited from suspension. Moreover, bed load is typically estimated to be only *ca.* 10% of the total load (Milliman & Farnsworth, 2011). Finally, denudation rates based on sediment yields take into account the solute loads carried by a river. In studies of ancient basins, it is impossible to estimate the solute load and therefore denudation rates are likely underestimated. However, solute loads in modern rivers typically are <20% of the total load except for rivers that drain landscapes dominated by periglacial processes (Berner & Berner, 1996; Milliman & Farnsworth, 2011).

## DISCUSSION

Ranges of sediment load and sediment–yield estimates for the Late Mississippian Pride–Glady Fork drainage system are compared to several well-studied modern rivers (Fig. 8; Table 3). At the first order, our estimates demonstrate that the Pride–Glady Fork paleoriver system was a high-sediment-flux system. The high sediment yields calculated for the Pride–Glady Fork basin are compatible with relatively high rates of erosion, a provenance of significant relief, and a climate characterized by seasonal, monsoonal discharge (Cecil, 1990; Miller & Eriksson, 1997, 1999). With the exception of the Indus River, load/yield data from the large drainage basin rivers are greater than even our maximum estimates for the Pride–Glady Fork system. While the Indus River data compares well with the minimum calculations and does have a similar climatic regime to the inferred paleoclimate of the Pride–Glady Fork, this estimate is precluded as the preferred value because: (1) paleogeographic reconstructions of

Blakey (2013) for the Upper Mississippian suggest relatively small drainage basins for transverse rivers originating from the fold-thrust belt to the east; and (2) the predominance of Appalachian-age zircons and the lack of mid-continent and Superior-age zircons in the underlying Princeton Formation are suggestive of a provenance akin to the fold-thrust belt to the east (Park *et al.*, 2010). Thus, modest drainage basin area estimates are favoured, similar to rivers such as the Fly and the Po and possibly as small as the Eel (Fig. 8; Table 3).

The calculated denudation rates for the Pride-Glady Fork drainage basin compare favourably with denudation rates determined for the modern Eel, Po, Fly, and Indus rivers (Table 3; Milliman & Farnsworth, 2011). Note that denudation rates for the other large drainage basin rivers are significantly higher than the Pride-Glady Fork estimate, which lends further support to the conclusion that the Pride-Glady Fork drainage basin was not as large as these systems. Generally, the smaller the drainage basin the less sediment storage occurs in up-system segments (Walling, 1983; Castellort & van den Driessche, 2003), and thus a closer relationship exists between sediment yield at the river mouth and denudation rate in the drainage basin. Recent debate about the relationship of sediment flux out of drainage basins to the denudation history in the same drainage basin (Warrick *et al.*, 2014; Willenbring *et al.*, 2014) further highlights the importance of evaluating the size and relief of the system in question. The approach for estimating denudation rates from stratigraphy presented in this study is not advised for larger (>ca. 100 000 km<sup>2</sup>) drainage basins because of appreciable sediment storage updip of river mouths.

An independent estimate of denudation rates for the Alleghanian Orogen based on flexural modelling of post-orogenic unloading (Jamieson & Beaumont, 1988) predicted up to 12 km of post-Alleghanian and pre-breakup erosion in the Inner Piedmont terrane of the Central Appalachians to the east of the Pride-Glady Fork depositor. If uplift commenced in the Mississippian and ended 100 million years later in the Triassic, denudation rates would have averaged on the order of 0.12 mm yr<sup>-1</sup>, which closely compares to our estimate of 0.116 mm yr<sup>-1</sup> for the moderate drainage basin area and median duration scenario. To what extent our sediment-yield-derived denudation rates are representative of the larger-scale Alleghanian orogen remains uncertain. Nevertheless, denudation rates derived from the sedimentary record can provide a quantitative measure of erosion-deposition dynamics at 10<sup>4</sup>–10<sup>5</sup> yr timescales that can be compared to other, widely used, techniques (e.g. thermochronometry) that typically capture exhumation and denudation at longer timescales.

## CONCLUSIONS

- (1) The rhythmically bedded Pride Shale preserves a hierarchy of tidal and climatic periodicities including

semi-diurnal, fortnightly and annual. Cycles in the Pride Shale represent high-resolution chronometers from which sedimentation rates of ca. 10 cm yr<sup>-1</sup> can be deduced.

- (2) Estimates of bankfull channel depths, based on thicknesses of architectural elements and cross sets in fluvial incised-valley and distributary-channel facies, used in conjunction with regional hydraulic curves, places constraints on catchment areas.
- (3) Sediment load, sediment yield, and suspended sediment concentration estimates for the Late Mississippian Pride-Glady Fork drainage system demonstrate that the paleoriver system was a high-sediment-flux system compatible with relatively high rates of erosion, a provenance of significant relief, and a climate characterized by seasonal, monsoonal discharge.
- (4) Integration of stratigraphic architectural analysis of the Pride Shale and stratigraphically adjacent units with a novel chronometric application highlights the utility of sedimentary archives as a record of Earth surface dynamics for ancient orogenic belts and adjoining sedimentary basins.

## ACKNOWLEDGEMENTS

Brian Turner, Jim Spotila, Mike Blum and one anonymous reviewer are acknowledged for their comments on earlier versions of this manuscript, and Ty Buller of ConocoPhillips is thanked for assistance with collection of channel dimension data in the field.

## SUPPORTING INFORMATION

Additional Supporting Information may be found in the online version of this article:

**Table S1.** Fluvial channel element thickness and cross-set thickness data.

## REFERENCES

- ALLEN, J.R.L. (1970) *Physical Processes of Sedimentation*. Allen and Unwin Ltd., London 248.
- ALLEN, P.A. (2008) Time scales of tectonic landscapes and their sediment routing systems. *Geol. Soc. Lond. Spec. Publ.*, **18**, 7–28.
- BAILY, R.J. & SMITH, D.G. (2010) Scaling in stratigraphic data series: implications for practical stratigraphy. *First Break*, **28**, 57–66.
- BERNER, R.A. & BERNER, E.K. (1996) *The Global Environment: Water, Air and Geochemical Cycles*. Prentice Hall, Upper Saddle River, NJ 376.
- BLAKEY, R. (2013) *Colorado Plateau Geosystems, Inc. Paleogeographic Maps*. <http://cpgeosystems.com/paleomaps.html>. Accessed 15 July 2014.

- BLUM, M., MARTIN, J., MILLIKEN, K. & GARVIN, M. (2013) Paleovalley systems: insights from Quaternary analogs and experiments. *Earth-Sci. Rev.*, **116**, 128–169.
- de BOER, P.L., OOST, A.P. & VISSER, M.J. (1989) The diurnal inequality of the tide as a parameter for recognizing tidal influences. *J. Sed. Petrol.*, **59**, 912–921.
- BRAUN, D.D. (1989) The depth of the post-middle Miocene erosion and the age of the present landscape. In: *The Rivers and Valleys of Pennsylvania, Then and Now* (Ed. by W.D. Sevon), pp. 16–20. Fieldtrip Guidebook, Harrisburg Area Geological Society Harrisburg, Harrisburg, PA.
- BRIDGE, J.S. & TYE, R.S. (2000) Interpreting the dimensions of ancient fluvial channel bars, channels, and channel belts from wireline-logs and cores. *Bull. Am. Assoc. Petrol. Geol.*, **84**, 1205–1228.
- BULLER, T.B. (2014) *Aspects of Cyclic Sedimentation in the Upper Mississippian, Mauch Chunk Group, Southern West Virginia and Southwest Virginia*. MS thesis, Virginia Tech, 148.
- CARRAPA, B. (2010) Resolving tectonic problems by dating detrital minerals. *Geology*, **38**, 191–192.
- CASTELLTORT, S. & van den DRIESSCHE, J. (2003) How plausible are high-frequency sediment supply-driven cycles in the stratigraphic record? *Sed. Geol.*, **157**, 3–13.
- CASTRO, J.M. & JACKSON, P.L. (2001) Bankfull discharge recurrence intervals and regional hydraulic geometry relationships: patterns in the Pacific Northwest, USA. *Am. Water Res. Assoc. J.*, **37**, 1249–1262.
- CECIL, C.B. (1990) Paleoclimatic controls on stratigraphic repetition of chemical and siliciclastic rocks. *Geology*, **18**, 533–536.
- CERVENY, P.F., NAESER, C.W., KELEMAN, P.B., LIEBERMAN, J.E. & ZEITLER, P.K. (1989) Zircon fission track ages from Gasherbrum Diorite, Karakorum Range, northern Pakistan. *Geology*, **17**, 1044–1048.
- COPELAND, P. & HARRISON, M.T. (1990) Episodic rapid uplift in the Himalaya revealed by  $^{40}\text{Ar}/^{39}\text{Ar}$  analysis of detrital K-feldspar and muscovite, Bengal Fan. *Geology*, **18**, 354–357.
- COVAULT, J.A., CRADDOCK, W.H., ROMANS, B.W., FILDANI, A. & GOSAL, M. (2013) Spatial and temporal variations in landscape evolution: historic and longer-term sediment flux through global catchments. *J. Geol.*, **121**, 35–56.
- DALRYMPLE, R.W., MAKINO, Y. & ZAITLIN, B.A. (1991) Temporal and spatial patterns of rhythmite deposition on mudflats in the macrotidal, Cobequid Bay–Salmon River estuary, Bay of Fundy, Canada. In: *Clastic Tidal Sedimentology* (Ed. by D.G. Smith, G.E. Reinson, B.A. Zaitlan & R.A. Rahmani), Can. Soc. Pet. Geol. Memoir, 16:137–160.
- DALRYMPLE, R.W., BAKER, E.K., HARRIS, P.T. & HUGHES, M.G. (2003) Sedimentology and stratigraphy of a tide-dominated, foreland-basin delta, Fly River, Papua New Guinea. *Tropical Deltas of Southeast Asia and Vicinity–Sedimentology, Stratigraphy, and Petroleum Geology. Soc. Econ. Paleont. Mineral. Spec. Publ.*, **76**, 147–173.
- DAVIDSON, S.K. & NORTH, C.P. (2009) Geomorphological regional curves for prediction of drainage area and screening modern analogues for rivers in the rock record. *J. Sed. Res.*, **79**, 773–792.
- ENGLUND, K.J. & THOMAS, R.E. (1990) Late Paleozoic depositional trends in the central Appalachian Basin. *U.S. Geol. Surv. Bull.*, **1839**, F1–F19.
- GRANGER, D.E. & SCHALLER, M. (2014) Cosmogenic nuclides and erosion at the watershed scale. *Elements*, **10**, 369–373.
- GREB, S.F., ARCHER, A.W. & de BOER, D.G. (2011) Apogean-perogean signals encoded in tidal flats at the fluvio-estuarine transition of Glacier Creek, Turnagain Arm, Alaska: implications for ancient tidal rhythmites. *Sedimentology*, **58**, 1434–1452.
- HARRIS, P.T., HUGHES, M.G., BAKER, E.K., DALRYMPLE, R.W. & KEENE, J.B. (2004) Sediment transport in distributary channels and its export to the pro-deltaic environment in a tidally dominated delta: Fly River, Papua New Guinea. *Cont. Shelf Res.*, **24**, 2431–2454.
- HOLBROOK, J. & WANAS, H. (2014) A fulcrum approach to assessing source-to-sink mass balance using channel paleohydrologic parameters derivable from common fluvial data sets with an example from the Cretaceous of Egypt. *J. Sed. Res.*, **84**, 349–372.
- HORI, K., SAITO, Y., ZHAO, Q. & WANG, P. (2002) Architecture and evolution of the tide-dominated Changjiang (Yangtze) River delta, China. *Sed. Geol.*, **146**, 249–264.
- HOYAL, D. & SHEETS, B. (2009) Morphodynamic evolution of experimental cohesive deltas. *J. Geophys. Res. Earth Surf.*, **114**, doi:10.1029/2007JF000882.
- HUBBARD, S.M., FILDANI, A., ROMANS, B.W., COVAULT, J.A. & MCHARGUE, T.R. (2010) High-relief slope clinoform development: insights from outcrop, Magallanes Basin, Chile. *J. Sed. Res.*, **80**, 357–375.
- JAEGER, J.M. & NITTROUER, C.A. (1995) Tidal controls on the formation of fine-scale sedimentary strata near the Amazon River mouth. *Mar. Geol.*, **125**, 259–281.
- JAMIESON, R.A. & BEAUMONT, C. (1988) Orogeny and metamorphism: a model for deformation and pressure-temperature-time paths with applications to the central and southern Appalachians. *Tectonics*, **7**, 417–445.
- KVALE, E.P. & ARCHER, A.W. (1991) Characteristics of two, Pennsylvanian-age, semi-diurnal tidal deposits in the Illinois Basin, USA. In: *Clastic Tidal Sedimentology* (Ed. by D.G. Smith, G.E. Reinson, B.A. Zaitlan & R.A. Rahmani), Can. Soc. Pet. Geol. Memoir, 16, 179–188.
- LARSEN, I.J., MONTGOMERY, D.R. & GREENBERG, H.M. (2014) The contribution of mountains to global denudation. *Geology*, **42**, 527–530.
- LIU, J.P., MILLIMAN, J.D., GAO, S. & CHENG, P. (2004) Holocene development of the Yellow River's subaqueous delta, North Yellow Sea. *Mar. Geol.*, **209**, 45–67.
- METIVIER, F. & GAUDEMER, Y. (1999) Stability of output fluxes of large rivers in South and East Asia during the last 2 million years. *Basin Res.*, **11**, 293–303.
- MIALL, A.D. (2015) Updating uniformitarianism: stratigraphy as just a set of 'frozen accidents'. *Geol. Soc. Lond. Spec. Publ.*, **404**, 11–36.
- MILLER, D.J. & ERIKSSON, K.A. (1997) Late Mississippian prodeltaic rhythmites in the Appalachian Basin: a hierarchical record of tidal and climatic periodicities. *J. Sed. Res.*, **B67**, 653–660.
- MILLER, D.J. & ERIKSSON, K.A. (1999) Linked sequence development and global climate change: the upper Mississippian record in the Appalachian basin. *Geology*, **27**, 35–38.
- MILLER, D.J. & ERIKSSON, K.A. (2000) Sequence stratigraphy of upper Mississippian strata in the Central Appalachians: a record of glacioeustasy and foreland-basin tectonics. *Bull. Am. Assoc. Petrol. Geol.*, **84**, 210–233.
- MILLIMAN, J.D. & FARNSWORTH, K.L. (2011) *River Discharge to the Coastal Ocean: A Global Synthesis*. Cambridge University Press, Cambridge 384.
- MOLNAR, P. & ENGLAND, P. (1990) Late Cenozoic uplift of mountain ranges and global climate change: Chicken or egg? *Nature*, **346**, 29–34.

- MULDER, T. & SYVITSKI, J.P.M. (1995) Turbidity currents generated at river mouths during exceptional discharges to the world oceans. *J. Geol.*, **103**, 285–299.
- MULDER, T., SYVITSKI, J.P.M., MIGEON, S., FAUGERES, J.-C. & SAVOYE, B. (2003) Marine hyperpycnal flows: initiation, behavior, and related deposits. A review. *Mar. Petrol. Geol.*, **20**, 861–882.
- OLARIU, C., STEEL, R.J. & PETTER, A.L. (2010) Delta-front hyperpycnal bed geometry and implications for reservoir modeling: Cretaceous Panther Tongue delta, Book Cliffs, Utah. *Bull. Am. Assoc. Petrol. Geol.*, **94**, 819–845.
- PAOLA, C. & BERGMAN, L. (1991) Reconstructing random topography from preserved stratification. *Sedimentology*, **38**, 553–565.
- PARK, H., BARBEAU, D.L., RICKENBAKER, A., BACHMANN-KRUG, D. & GEHRELS, G. (2010) Application of foreland basin detrital-zircon geochronology to the reconstruction of the southern and central Appalachian Orogen. *J. Geol.*, **118**, 23–44.
- PATRUNO, S., HAMPSON, G.J. & JACKSON, C.A.L. (2015) Quantitative characterization of deltaic and subaqueous clinoforms. *Earth Sci. Rev.*, **142**, 79–119.
- PLOTNICK, R.E. (1986) A fractal model for the distribution of stratigraphic hiatuses. *J. Geol.*, **94**, 885–890.
- POAG, C.W. & SEVON, W.D. (1989) A record of Appalachian denudation in postrift Mesozoic and Cenozoic deposits of the US middle Atlantic Continental Margin. *Geomorphology*, **2**, 119–157.
- PORTENGA, E.W. & BIERMAN, P.R. (2011) Understanding Earth's eroding surface with <sup>10</sup>Be. *GSA Today*, **21**, 4–10.
- PRIOR, D.B., YANG, Z.-S., BORNHOLD, B.D., KELLER, G.H., LU, N.Z., WISEMAN, W.J. Jr, WRIGHT, L.D. & ZHANG, J. (1986) Active slope failure, sediment collapse, and silt flows on the modern subaqueous Haunghe (Yellow River) delta. *Geo-Mar. Lett.*, **6**, 85–95.
- REED, J.S., ERIKSSON, K.A. & KOWALEWSKI, M. (2005a) Controls on Carboniferous sandstone diagenesis, Central Appalachian basin: a qualitative and quantitative assessment. *Sed. Geol.*, **176**, 225–246.
- REED, J.S., SPOTILA, J.A., ERIKSSON, K.A. & BODNAR, R.J. (2005b) The downs and ups of Pennsylvanian strata, central Appalachian basin. *Basin Res.*, **17**, 259–268.
- RESENTINI, A. & MALUSA, M.G. (2012) Sediment budgets by detrital apatite fission-track dating (Rivers Dora Baltea and Arc, Western Alps). In: *Mineralogical and Geochemical Approaches to Provenance* (Ed. by E.T. Rastbury, S.R. Hemming & N.R. Riggs) Geological Society of America Special Paper 487, 125–140, doi: 10.1130/2012.2487(08).
- ROMANS, B.W. & GRAHAM, S.A. (2013) A deep-time perspective on land-ocean linkages in the sedimentary record. *Ann. Rev. Mar. Sci.*, **5**, 69–94.
- ROMANS, B.W., CASTELLTORT, S., COVAULT, J.A., FILDANI, A. & WALSH, J.P. (2015) Environmental signal propagation in sedimentary systems across timescales. *Earth Sci. Rev.*, doi: 10.1016/j.earscirev.2015.07.012.
- SADLER, P.M. (1981) Sediment accumulation rates and the completeness of stratigraphic sections. *J. Geol.*, **89**, 569–584.
- SADLER, P.M. & JEROLMACK, D.J. (2015) Scaling laws for aggradation, denudation, and progradation rates: the case for time-scale invariance at sediment sources and sinks. *Geol. Soc. Lond. Spec. Publ.*, **404**, 69–88.
- SORKHABI, R.B., STUMP, E., FOLAND, K.A. & JAIN, A.K. (1996) Fission-track and <sup>40</sup>Ar/<sup>39</sup>Ar evidence for episodic denudation of the Gangotri granites in the Garhwal Higher Himalaya, India. *Tectonophysics*, **260**, 187–199.
- TESSIER, B. (1993) Upper intertidal rhythmites in the Mont-Saint-Michel Bay (NW France): perspectives for paleoreconstruction. *Mar. Geol.*, **110**, 355–367.
- WALLING, D.E. (1983) The sediment delivery problem. *J. Hydrol.*, **65**, 209–237.
- WARRICK, J.A., MILLIMAN, J.D., WALLING, D.E., WASSON, R.J., SYVITSKI, J.P.M. & AALTO, R.E. (2014) Earth is (mostly) flat: apportionment of the flux of continental sediment over millennial time scales: COMMENT. *Geology*, **42**, e316.
- WILLENBRING, J.K. & von BLANCKENBURG, F. (2010) Long-term stability of global erosion rates and weathering during late-Cenozoic cooling. *Nature*, **465**, 211–214.
- WILLENBRING, J.K., CODILEAN, A.T. & MCELROY, B. (2014) Earth is (mostly) flat: apportionment of the flux of continental sediment over millennial time scales: REPLY. *Geology*, **42**, e317.
- WILLIAMS, G.E. (1989) Late Precambrian tidal rhythmites in South Australia and the history of the Earth's rotation. *Jour. Geol. Soc. London*, **146**, 97–111.
- WILLIAMS, G.E. (1991) Upper Proterozoic tidal rhythmites, South Australia: sedimentary features, deposition, and implications for the earth's paleorotation. In: *Clastic Tidal Sedimentology* (Ed. by D.G. Smith, G.E. Reinson, B.A. Zaitlan & R.A. Rahmani), Can. Soc. Pet. Geol. Memoir, **16**, 161–177.
- ZEITLER, P.K., HERCZEG, A., MCDUGALL, I. & HONDA, M. (1987) U-Th-He dating of apatite: a potential thermochronometer. *Geochim. Cosmochim. Acta*, **51**, 2865–2868.

*Manuscript received 6 February 2015; In revised form 20 August 2015; Manuscript accepted 24 September 2015.*